

# Small potent ligands to the insulin-regulated aminopeptidase (IRAP)/AT<sub>4</sub> receptor

ANDREAS AXÉN,<sup>a</sup> HANNA ANDERSSON,<sup>a</sup> GUNNAR LINDBERG,<sup>a</sup> HARRIET RÖNNHOLM,<sup>c</sup> JARKKO KORTESMAA,<sup>c</sup> HEIDI DEMAEGDT,<sup>b</sup> GEORGES VAUQUELIN,<sup>b</sup> ANDERS KARLÉN<sup>a</sup> and MATHIAS HALLBERG<sup>d\*</sup>

<sup>a</sup> Department of Medicinal Chemistry, Uppsala University, Box 574, SE-751 23 Uppsala, Sweden

<sup>b</sup> Department of Molecular and Biochemical Pharmacology, Vrije Universiteit Brussel, Pleinlaan 2, 1050 Brussels, Belgium

<sup>c</sup> Neuronova AB, Fiskartorpsvägen 15C, SE-11433 Stockholm, Sweden

<sup>d</sup> Department of Pharmaceutical Biosciences, Uppsala University, Box 591, SE-751 24 Uppsala, Sweden

Received 4 March 2007; Accepted 10 March 2007

**Abstract:** Angiotensin IV analogs encompassing aromatic scaffolds replacing parts of the backbone of angiotensin IV have been synthesized and evaluated in biological assays. Several of the ligands displayed high affinities to the insulin-regulated aminopeptidase (IRAP)/AT<sub>4</sub> receptor. Displacement of the C-terminal of angiotensin IV with an *o*-substituted aryl acetic acid derivative delivered the ligand **4**, which exhibited the highest binding affinity ( $K_i = 1.9$  nM). The high affinity of this ligand provides support to the hypothesis that angiotensin IV adopts a  $\gamma$ -turn in the C-terminal of its bioactive conformation.

Ligand (**4**) inhibits both human IRAP and aminopeptidase N-activity and induces proliferation of adult neural stem cells at low concentrations. Furthermore, ligand **4** is degraded considerably more slowly in membrane preparations than angiotensin IV. Hence, it might constitute a suitable research tool for biological studies of the (IRAP)/AT<sub>4</sub> receptor. Copyright © 2007 European Peptide Society and John Wiley & Sons, Ltd.

**Keywords:** angiotensin IV; insulin-regulated aminopeptidase; IRAP; structure–activity relationship; peptide synthesis; peptidomimetic; turn mimetic; bioactive conformation; adult neural stem cells

## INTRODUCTION

There are many examples of enzymatic processing of neuropeptides, in which the conversion products exhibit different biological effects as compared to the native peptide from which they are derived [1,2]. Angiotensin IV (Ang IV; Val-Tyr-Ile-His-Pro-Phe) (**1**), one of the bioactive degradation products in the renin–angiotensin system, constitutes one example of a metabolite that frequently exerts effects other than those of its precursors [3–5]. The observations that the hexapeptide possesses an inherent ability to facilitate learning and memory in behavioral models have attracted considerable interest in recent years [6–13]. Ang IV is known to stimulate DNA synthesis and enhance thymidine incorporation [14] and is probably

at some level engaged in a number of neurobiological actions including neural development and neuron survival.

The Ang IV receptor, first described as the specific high-affinity binding site for Ang IV [15], was recently identified as a transmembrane enzyme, the IRAP (EC 3.4.11.3), and abundantly occurs in vesicles with the insulin-sensitive glucose transporter GLUT4 [16]. IRAP is a cystine aminopeptidase and belongs to the M1 family of zinc-dependent metallo-peptidases [17]. It is suggested that Ang IV receptor ligands act by binding to IRAP inhibiting the catalytic activity [18]. It has been proposed that Ang IV ligands at least partly exert their actions by prolonging the half-life of one or more of the neuropeptides that are known to serve as substrates to IRAP and are recognized for their ability to facilitate learning and memory [3,16]. It has also been proposed that IRAP may have signaling capabilities that are not dependent on the protease activity or that there might be additional, yet unidentified receptor(s) for Ang IV (for a review, see [19]). It is argued that to trigger an effect through accumulation of IRAP, substrate peptides should take considerable time but, on the contrary, several studies have described both physiological effects [20,21] and a large variety of intracellular signaling events [22–24] triggered by Ang IV peptides which manifest within a few minutes or even faster. Furthermore, the minimal effective ligand concentrations are below those required for other enzyme inhibitors [22–24]. Regardless of the open questions

Abbreviations: AP-N, aminopeptidase N; Boc, *tert*-butyloxycarbonyl; *t*-Bu, *tert*-butyl; BSA, bovine serum albumin; DCM, dichloromethane; DMF, *N,N*-dimethylformamide; DMSO, dimethyl sulfoxide; Cha, cyclohexylalanine; Fmoc, 9-fluorenylmethyloxycarbonyl; HBTU, 2-(1H-benzotriazole-1-yl)-1,1,3,3-tetramethyluronium hexafluorophosphate; Hcy, homocysteine; IRAP, insulin-regulated aminopeptidase; *L*-Leu-pNA, *L*-leucine-*p*-nitroanilide; NMM, *N*-methylmorpholine; 1,10-Phe, 1,10-phenanthroline; PDMS, plasma desorption mass spectrometry; PMSF, phenyl methyl sulfonyl fluoride; RP-HPLC, reversed phase high-performance liquid chromatography; TFA, trifluoroacetic acid; Trt (trityl), triphenylmethyl.

\*Correspondence to: M. Hallberg, Department of Pharmaceutical Biosciences, Division of Biological Research on Drug Dependence, Uppsala University, SE-751 24 Uppsala, Sweden; e-mail: Mathias.Hallberg@farmbio.uu.se

that remain concerning the signaling mechanism(s) and the existence of additional receptor(s), the Ang IV/IRAP interaction is well established [16,25,26].

The structure–activity relationships of linear peptidic Ang IV analogs have been studied in detail [27–30]. In efforts to determine the bioactive conformation of Ang IV when it binds to the IRAP/AT<sub>4</sub> receptor, we recently examined a series of nonlinear constrained peptide analogs encompassing macrocyclic disulfide systems [31]. It was found that replacement of the C-terminal tripeptide His-Pro-Phe by Cys-Pro-Cys and subsequent oxidative cyclization rendered a ligand (**2**) essentially equipotent to the native hexapeptide, despite lacking both the imidazole and phenyl rings of the His<sup>4</sup> and Phe<sup>6</sup> residues. As deduced from a conformational analysis, the C-terminal of this cyclic Ang IV analog was concluded to preferably adopt a  $\gamma$ -turn [31]. This observation encouraged us to replace the C-terminal tripeptide with structurally simple and properly substituted benzoic acids and phenyl acetic acids with the primary objective to mimic the constrained  $\gamma$ -turn, inducing a cyclic system with its C-terminal carboxylate group. Such designed peptidomimetics are more drug-like and should be metabolically more stable *in vivo* and consequently, provided that they are reasonable potent binders, could be expected to serve as valuable research tools in animal models.

A novel treatment paradigm termed *therapeutic neurogenesis* has been envisioned for neurodegenerative diseases such as Parkinson's and Huntington's as well as for depression. In essence, the patient's endogenous neural stem cells are pharmaceutically stimulated to generate new cells (for a review, see Ref. 32). In some cases, the new cells may have the potential to replace the function of the neurons lost owing to the disease. Equally importantly, several lines of evidence suggest that new cells, derived from the neural stem cells, may have therapeutic potential through other mechanisms, such as production of neuroprotective/neurotrophic factors or modulation of the immune system (for examples, see Refs 33,34). To realize the concept, it is of interest to elucidate the mechanisms and receptors that govern the proliferation of adult neural stem cells. In light of the well-known effects of the Ang IV peptide in brain, IRAP/AT<sub>4</sub> is an interesting, but not-well-understood molecular candidate with a potential role in stem cell proliferation.

We herein report that incorporation of an aromatic scaffold as substitute for the backbone of the three amino acid residues of the C-terminal of Ang IV can deliver potent IRAP/AT<sub>4</sub> receptor ligands. The most potent ligand in the series, compound **4**, with a  $K_i$  value of 1.9 nM, inhibits the enzyme activity of human IRAP and AP-N as efficiently as Ang IV. Furthermore, we also report that compound **4** induces proliferation of adult neural stem cells expressing the IRAP/AT<sub>4</sub> receptor.

## MATERIALS AND METHODS

### Materials

Fmoc-Phe Wang resin, Rink amide MBHA resin and amino acid derivatives were obtained from Bachem (Bubendorf, Switzerland) or Novabiochem (Läufelfingen, Switzerland). 2-Cl-tritylchloride resin was the product of Alexis Corporation (Läufelfingen, Switzerland). Fmoc-amino acids were loaded onto this resin as described in the literature [35]. Fmoc-3-aminomethylbenzoic acid was obtained from Neosystems. HBTU was obtained from Senn Chemicals (Dielsdorf, Switzerland). DMF (analytical grade) was provided by Fischer Chemicals (Loughborough, UK) and was used without further purification. L-Leu-pNA and L-alanine-p-nitroanilide were obtained from Sigma-Aldrich (Bornem, Belgium) and *p*-nitroaniline from VWR International (Leuven, Belgium). Tyr<sup>4</sup> of Ang IV was iodinated using the Iodogen iodination reagent from Pierce (Erembodegem, Belgium) as described in Ref. 36. <sup>125</sup>I was obtained from MP Biomedicals (Asse, Belgium). Monoiodinated Ang IV was isolated on a GraceVydac C18 monomeric 120A reverse-phase HPLC column and stored at –20 °C in 10 mM KH<sub>2</sub>PO<sub>4</sub>, pH 6.5 containing 45% ethanol. All other reagents were of the highest grade commercially available. CHO-K1 cells were obtained from the Pasteur Institute (Brussels, Belgium). Mass spectroscopy was carried out on an Applied Biosystems (Uppsala, Sweden) BIOION 20 PDMS. Amino acid analyses were performed at the Department of Biochemistry, Uppsala University, Sweden, using an LKB 4151 alpha plus analyzer with ninhydrin detection. Samples were hydrolyzed with 6 M HCl at 110 °C for 24 h.

### General Procedure for Solid-Phase Peptide Synthesis (SPPS) and Purification

Unless otherwise stated, the peptides were synthesized on a 100- $\mu$ mol scale with a Symphony instrument (Protein Technologies Inc., Tucson, AZ, USA) using Fmoc/*t*-Bu protection. The following side-chain-protected derivatives were used: Fmoc-Tyr(*t*-Bu) and Fmoc-His(Trt) or Fmoc-His(Boc). Removal of the Fmoc group was achieved by reaction with 20% piperidine in DMF (2  $\times$  2.5 ml) for 5 + 10 min. Coupling of the amino acids (125  $\mu$ mol) was performed in DMF (2.5 ml) using HBTU (125  $\mu$ mol) in the presence of NMM (500  $\mu$ mol). Double couplings (2  $\times$  30 min) were used for all amino acids. After introduction of each amino acid, the remaining amino groups were capped by addition of 20% acetic anhydride in DMF (1.25 ml) to the coupling mixture and allowing the reaction to proceed for 5 min. After completion of the synthesis, the Fmoc group was removed and the partially protected peptide resin was washed with several portions of DMF and DCM and dried in a stream of nitrogen and *in vacuo*.

Manual SPPS was carried out in a similar way using disposable syringes (2 or 5 ml capacity) fitted with porous polyethylene filters as reaction vessels. Peptides were cleaved and deprotected by treatment with TFA–H<sub>2</sub>O–triethylsilane (90:5:5; ca 2 ml/100 mg resin) for 1.5–2 h. The resin was filtered off and washed with TFA. The combined filtrates, collected in a centrifuge tube, were concentrated and the product was precipitated by the addition of cold ether. The crude peptide was then collected by centrifugation, washed with several portions of ether and dried. Part of the crude peptide (ca 25 mg) was dissolved in 0.1%

TFA–10% CH<sub>3</sub>CN–H<sub>2</sub>O (2.2 ml), filtered through a 0.45- $\mu$ m nylon membrane and purified by RP-HPLC. Unless otherwise indicated, preparative RP-HPLC was performed on a Vydac 10  $\mu$ m C18 column (22  $\times$  250 mm) using gradients of CH<sub>3</sub>CN in 0.1% aqueous TFA at a flow rate of 3 ml/min and detection at 230 nm. Analytical RP-HPLC was performed on a Vydac 10  $\mu$ m C18 column (4.6  $\times$  150 mm) using detection at 220 nm.

Selected fractions were analyzed by RP-HPLC and/or PDMS. Those containing the pure material were pooled, lyophilized and dissolved in water (occasionally supplemented with CH<sub>3</sub>CN). The peptide content, usually 70–80% on a weight basis, was then determined by amino acid analysis of a withdrawn aliquot.

## Products

**Val-Tyr-Ile-His-Pro-Phe (1).** The peptide (Ang IV) was prepared according to the standard SPPS protocol. The final yield was 25.2 mg (32.5%). PDMS ( $M_w$  774.9): 775.9 (M + H<sup>+</sup>); amino acid analysis: Val, 0.97; Tyr, 1.00; Ile, 0.91; His, 0.90; Pro, 1.03; Phe, 1.00 (75.8% peptide).

**Val-Tyr-Ile-His-Pro-Phe-NH<sub>2</sub> (3).** The amide was synthesized manually from Rink amide MBHA resin on a 30- $\mu$ mol scale. The final yield was 9.1 mg (39.0%). PDMS ( $M_w$  773.9): 774.9 (M + H<sup>+</sup>); amino acid analysis: Val, 0.99; Tyr, 1.00; Ile, 0.93; His, 0.92; Pro, 1.00; Phe, 1.01 (73.1% peptide).

**2-Azidomethylphenylacetyl-2-Cl-trityl resin.** 2-Azidomethylphenylacetic acid [37,38] (0.52 mmol) was reacted with 2-Cl-tritylchloride resin (0.79 mmol) according to the literature procedure [35]. The coupling was monitored by HPLC analysis of the liquid phase and was essentially complete (97%) after 3 h. According to the weight increase, the resulting substitution degree was 0.84 mmol/g.

**Fmoc-Ile-2-aminomethylphenylacetyl-2-Cl-trityl resin.** The title compound was obtained by a slightly modified literature procedure [37]. A mixture of Fmoc-Ile-OH (477 mg, 1.35 mmol), HOBt (182 mg, 1.35 mmol) and diisopropylcarbodiimide (212  $\mu$ l, 1.35 mmol) in dry DCM (25 ml) was preactivated in a nitrogen atmosphere for 10 min. 2-Azidomethylphenylacetyl-2-Cl-trityl resin (533 mg, 0.45 mmol) was added to the solution, followed after 1 min by tributylphosphine (260  $\mu$ l, 0.90 mmol). The mixture was stirred under nitrogen for 2 h. The resin was then filtered off, washed with DCM, DMF, MeOH and DCM and dried to yield 668 mg of the desired resin.

**Val-Tyr-Ile-2-aminomethylphenylacetic acid (4).** Fmoc-Ile-2-aminomethylphenylacetyl-2-Cl-trityl resin (0.45 mmol) was elongated by deprotection and coupling of, in turn, Fmoc-Tyr(*t*-Bu)-OH and Fmoc-Val-OH (3 equiv.) using HBTU (3 equiv.) and DIEA (6 equiv.) and a reaction time of 2 h. Part of the deprotected, washed and dried resin (154 mg, 108  $\mu$ mol) was reacted with TFA–H<sub>2</sub>O–triethylsilane to yield the crude product (41.2 mg). After purification by RP-HPLC using an ACE 5 Phenyl column (21.2  $\times$  150 mm) 27.8 mg (47.9%) of the desired compound were recovered. LC-MS ( $M_{abs}$  540.2947): 541.2 (M + H<sup>+</sup>); amino acid analysis: Val, 0.99; Tyr, 1.01; Ile, 0.72; 2-aminomethylphenylacetic acid, 0.72 (79.8% peptide).

**3-Bromomethylphenylacetic acid.** 3-Tolylacetic acid (3.0 g, 20 mmol), *N*-bromosuccinimide (3.7 g, 21 mmol) and benzoylperoxide (100 mg) were dissolved in 150 ml of CCl<sub>4</sub>. The mixture was refluxed for 15 h and filtered hot. The filtrate was concentrated *in vacuo*. The solid was purified on a silica column eluted with pentane–ether (2 : 8). The appropriate fractions were collected and concentrated, followed by crystallization from ether–pentane. White solid, 1.65 g (54%). <sup>1</sup>H NMR (270 MHz, CDCl<sub>3</sub>)  $\delta$  11.12 (s, 1H, COOH), 7.35–7.15 (m, 4H, ar), 4.48 (s, 2H, CH<sub>2</sub>-Br), 3.68 (s, 2H, CH<sub>2</sub>-COOH). <sup>13</sup>C NMR (270 MHz, CDCl<sub>3</sub>)  $\delta$  77.8, 138.3, 134.0, 130.0, 129.5, 129.1, 128.1, 40.7, 33.1. IR (KBr); 3025, 1696, 1401, 1219 cm<sup>-1</sup>. Elemental analysis: calc. for C<sub>9</sub>H<sub>9</sub>BrO<sub>2</sub>: C, 47.19%; H, 3.96%; obtained: C, 47.5%; H, 4.0%.

**Fmoc-3-aminomethylphenylacetic acid.** 3-Bromomethylphenylacetic acid (1.15 g, 5 mmol) was dissolved in 100 ml of ethanol and ammonia was bubbled through the solution for 30 min. The solution was stirred at room temperature for 30 min and then evaporated to dryness. The remaining solid was dissolved in a mixture of 25 ml of 10% sodium carbonate and 10 ml of dioxane. This solution was cooled to 0°C and a solution of Fmoc-Cl (1.55 g, 6 mmol) in 15 ml of dioxane was added in portions over a period of 30 min. The mixture was stirred for 4 h at 0°C, followed by 15 h of stirring at room temperature. The mixture was diluted with 200 ml of water and the pH was adjusted to ca 1 with 2 M HCl. The aqueous phase was extracted with four 30 ml portions of DCM, the combined organic phases were dried and the solvent was removed *in vacuo*. Recrystallization from ethyl acetate–diethylether–pentane yielded 1.3 g (67%) of a white solid. <sup>1</sup>H NMR (270 MHz, d<sub>6</sub>-DMSO)  $\delta$  12.5 (s, 1H, COOH), 8.0–7.65 (m, 4H, ar), 7.5–7.0 (m, 8H, ar-Fmoc), 4.4–4.1 (m, CH-Fmoc, 6H, CH<sub>2</sub>-Fmoc, NH, CH<sub>2</sub>-N), 3.55 (s, 2H, CH<sub>2</sub>-COOH). <sup>13</sup>C NMR (270 MHz, d<sub>6</sub>-DMSO)  $\delta$  172.6, 156.3, 143.9, 140.7, 139.7, 135.0, 128.2, 127.9, 127.8, 127.6, 125.2, 125.1, 120.1, 65.3, 46.7, 43.6. IR (KBr); 3307, 3036, 1695, 1531, 1266 cm<sup>-1</sup>. PDMS ( $M_w$  385.5): 387.0 (M + H<sup>+</sup>) Elemental analysis: calc. for C<sub>24</sub>H<sub>21</sub>NO<sub>4</sub>: C, 74.40%; H, 5.46%; N, 3.62%; O, 16.5%; obtained: C, 73.9%; H, 5.7%; N, 3.7%; O, 16.6%.

**Val-Tyr-Ile-3-aminomethylphenylacetic acid (5).** This substance was synthesized from Fmoc-3-aminomethylphenylacetic acid (200  $\mu$ mol) attached to 2-Cl-trityl resin following the procedure described for **4** above. Yield: 11.8 mg (10.9%). PDMS ( $M_w$  540.6): 541.0 (M + H<sup>+</sup>); amino acid analysis: Val, 1.01; Tyr, 1.00; Ile, 0.97; 3-aminomethylphenylacetic acid, 1.02 (78.5% peptide).

**Val-Tyr-Ile-3-aminomethylbenzoic acid (6).** The compound was prepared from Fmoc-3-aminomethylbenzoic acid (200  $\mu$ mol) attached to 2-Cl-trityl resin as described above. Yield: 10.8 mg (10.3%). PDMS ( $M_w$  526.6): 528.0 (M + H<sup>+</sup>); amino acid analysis: Val, 0.99; Tyr, 0.99; Ile, 0.97; 3-aminobenzoic acid, 1.05 (76.5% peptide).

***N*-Phthaloyl-4-aminomethylphenylacetic acid.** Phenylacetic acid (2.1 g, 150 mmol) and *N*-(hydroxymethyl)phthalimide (2.6 g, 150 mmol) were dissolved in 20 ml of TFA and refluxed for 48 h. The solvent was removed *in vacuo* and the remaining solid was purified by column chromatography (silica, diethyl ether). The appropriate fractions were collected and the solvent was removed *in vacuo* yielding a white solid

(2.5 g, 54%). This material was a mixture of the *p*- and *o*-isomer of *N*-phthaloylaminomethylphenylacetic acid. The pure *p*-isomer could be isolated by fractional crystallization (chloroform–diethyl ether) in reasonable yields (0.5–0.8 g). <sup>1</sup>H NMR (270 MHz, CDCl<sub>3</sub>) δ 7.86–7.67 (m, 4H, ar. phthalimide), 7.42–7.27 (m, 4H, ar), 4.82 (s, 2H, CH<sub>2</sub>-NH), 3.60 (s, 2H, CH<sub>2</sub>-COOH). <sup>13</sup>C NMR (270 MHz, CDCl<sub>3</sub>) δ 76.8, 168.1, 135.5, 134.0, 132.9, 132.1, 129.7, 129.1, 123.4, 41.3, 40.6. IR (KBr) 3001, 2942, 1719, 1707, 1425, 1384 cm<sup>-1</sup>.

**Fmoc-4-aminomethylphenylacetic acid.** *N*-Phthaloyl-4-aminomethylphenylacetic acid (295 mg, 1 mmol) was dissolved in 50 ml of ethanol, and hydrazine hydrate (50 mg, 1 mmol) was added. After 15 h of reflux, a second portion of hydrazine hydrate (10 mg, 0.2 mmol) was added and the reflux was continued for an additional 5 h. The solvent was removed *in vacuo* and the remaining solid was dissolved in a mixture of 20 ml of 10% sodium carbonate and 10 ml of dioxane. This solution was cooled to 0 °C and a solution of Fmoc-Cl (518 mg, 2 mmol) in 10 ml of dioxane was added in portions over a period of 30 min. The mixture was stirred for 4 h at 0 °C, followed by 48 h at room temperature. The mixture was diluted with 100 ml of water and the pH was adjusted to *ca* 1 with 2 M HCl. The aqueous phase was extracted with four 20 ml portions of DCM, the organic phases were dried and the solvent was removed *in vacuo*. The solid was purified on a silica column, eluted with diethyl ether followed by ethyl acetate and finally by 20% acetic acid in ethyl acetate. The material eluted with acetic acid/ethyl acetate was collected, the solvent volume reduced *in vacuo* to approximately 2 ml, and the product precipitated with diethyl ether to yield 150 mg (30%) as an off-white solid. <sup>1</sup>H NMR (270 MHz, *d*<sub>6</sub>-DMSO) δ 13.5 (s, 1H, COOH), 7.9–7.25 (m, 8H, ar-Fmoc), 7.2–7.05 (m, 4H, ar), 4.32 (d, 2H, CH<sub>2</sub>-Fmoc), 4.23 (d, 1H, NH), 4.21 (t, 1H, CH-Fmoc), 4.12 (d, 2H, CH<sub>2</sub>-N), 3.32 (s, 2H, CH<sub>2</sub>-COOH). <sup>13</sup>C NMR (270 MHz, *d*<sub>6</sub>-DMSO) δ 174.1, 156.3, 143.8, 140.7, 137.1, 129.1, 127.5, 127.0, 126.5, 125.1, 120.0, 65.4, 46.9, 43.3, 22.7. IR (KBr): 3307, 3036, 1689, 1537, 1255 cm<sup>-1</sup>.

**Val-Tyr-Ile-4-aminomethylphenylacetic acid (7).** The product was obtained from Fmoc-Val-Tyr-Ile-4-aminomethylphenylacetic acid (200 μmol) attached to 2-Cl-trityl resin according to the above procedure. Yield: 16.9 mg (15.6%). PDMS (*M*<sub>w</sub> 540.6): 542.1 (M + H<sup>+</sup>); amino acid analysis: Val, 1.02; Tyr, 0.98; Ile, 0.77; 4-aminomethylphenylacetic acid, 0.81 (100% peptide).

**Val-Tyr-Ile-7-aminoheptanoic acid (8).** Fmoc-7-aminoheptanoic acid (100 μmol) was loaded onto a 2-Cl-trityl resin as described in the literature [35]. The remaining amino acids (2 equiv.) were coupled manually using HBTU (2 equiv.) as activating agent and NMM (4 equiv.) as base. After removal of the Fmoc group, the product was deprotected and cleaved from the resin by treatment with 3 ml TFA–H<sub>2</sub>O–triethylsilane (90 : 5 : 5) for 1.5 h. Yield of purified product: 23.0 mg (44.2%). PDMS (*M*<sub>w</sub> 520.6): 522.1 (M + H<sup>+</sup>); amino acid analysis: Val, 0.99; Tyr, 1.02; Ile, 0.66; 7-aminoheptanoic acid, 0.77 (73.6% peptide).

**3-Aminomethyl-5-(4'-hydroxybenzyl)benzoyl-His-Pro-Phe (10).** The substance was prepared on a 38-μmol scale from Fmoc-3-aminomethyl-5-(4'-Fmoc-oxybenzyl)benzoic acid [39] and His(Trt)-Pro-Phe-Wang resin using coupling with

PyBOP/DIEA for 17 h. Fmoc removal, cleavage with TFA–H<sub>2</sub>O–triethylsilane and purification by RP-HPLC gave 13.4 mg (55.2%). PDMS (*M*<sub>w</sub> 638.8): 639.9 (M + H<sup>+</sup>); amino acid analysis: His, 1.00; Pro, 1.00; Phe, 1.00; 3-aminomethyl-5-(4'-hydroxybenzyl)benzoic acid, n.d. (70.3% peptide).

**3-Aminomethyl-5-(4'-hydroxybenzyl)benzoyl-Ile-His-Pro-Phe (11).** This compound was synthesized and purified as above but using Ile-His(Trt)-Pro-Phe-Wang resin as the starting material. The yield was 11.4 mg (39.3%). PDMS (*M*<sub>w</sub> 751.9): 752.2 (M + H<sup>+</sup>); amino acid analysis: Ile, 0.96; His, 1.02; Pro, 0.99; Phe, 1.03; 3-aminomethyl-5-(4'-hydroxybenzyl)benzoic acid, n.d. (68.4% peptide).

### Cell Culture, Transient Transfection and Membrane Preparation

CHO-K1 and HEK293 cell lines were cultured in 75 and 500 cm<sup>3</sup> culture flasks in Dulbecco's modified essential medium (DMEM) supplemented with L-glutamine (2 mM), 2% (v/v) of a stock solution containing 5000 IU/ml penicillin and 5000 μg/ml streptomycin (Invitrogen, Merelbeke, Belgium), 1% (v/v) of a stock solution containing nonessential amino acids, 1 mM sodium pyruvate and 10% (v/v) fetal bovine serum (Invitrogen, Merelbeke, Belgium). The cells were grown in 5% CO<sub>2</sub> at 37 °C until confluent.

HEK293 cells were transiently transfected with plasmid DNA, pCIneo containing the gene of human IRAP (kindly provided by Prof. M. Tsujimoto, Laboratory of Cellular Biochemistry, Saitama, Japan) or pTEJ4 [40] carrying the complete human AP-N cDNA [41]. The transient transfection was performed as described previously with 8 μl/ml LipofectAMINE (Invitrogen, Merelbeke, Belgium) and 1 μg/ml plasmid DNA [42]. After transfection, the cells were cultured for two more days. IRAP and AP-N transfected HEK293 cells displayed 10 and 8 times higher enzyme activity than nontransfected cells, respectively.

CHO-K1 cell and transfected HEK293 cell membranes were prepared as described previously [26]. In short, the cells were harvested with 0.2% EDTA (w/v) (in PBS, pH 7.4) and centrifuged for 5 min at 500 *g* at room temperature. After resuspending in PBS, the number of cells were counted and washed. The cells were then homogenized in 50 mM Tris-HCl (at pH 7.4) using a Polytron (10 s at maximum speed) and Potter homogenizer (30 strokes at 1000 rpm) and then centrifuged for 30 min (30 000 *g* at 4 °C). The pellet was resuspended in 50 mM Tris-HCl and centrifuged (30 min 30 000 *g* at 4 °C), and the supernatant was removed. The resulting pellets were stored at –20 °C until use.

For the preparation of porcine frontal cortex membranes, the cortical tissue was homogenized in 40 volumes of 50 mM Tris-HCl, 5 mM EDTA buffer (pH 7.4) using a Polytrone homogenizer. The homogenate was centrifuged (500 *g* at 4 °C) for 10 min and the supernatant was recentrifuged (40 000 *g* at 4 °C) for 20 min. The pellet was dissolved in 40 volumes of 50 mM Tris-HCl, 5 mM EDTA buffer and subsequently homogenized and recentrifuged (40 000 *g*) for another 20 min. The final pellet was dissolved in 25 volumes of 50 mM Tris-HCl, 5 mM EDTA buffer, homogenized, aliquoted and kept at –80 °C until further use.

## Enzyme Assay

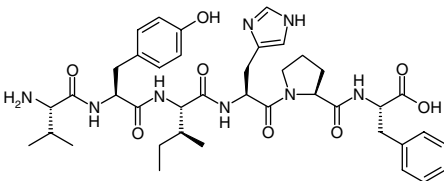
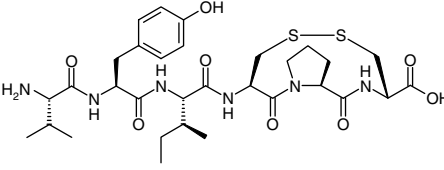
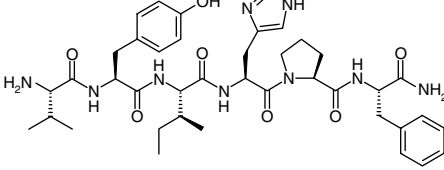
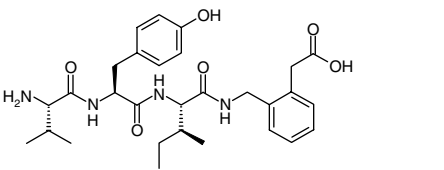
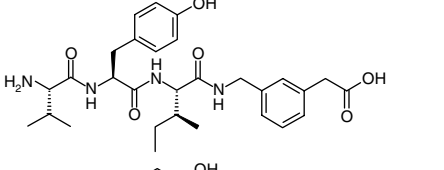
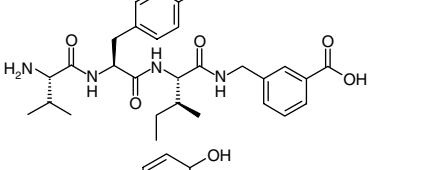
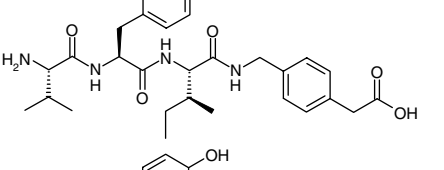
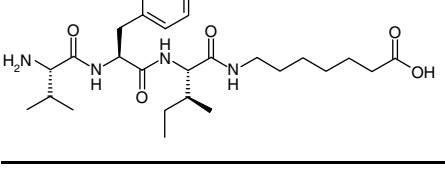
Determination of the aminopeptidase catalytic activity was based on the cleavage of the substrate L-Leu-pNA [26] into L-leucine and *p*-nitroaniline. This latter compound displays a characteristic absorption maximum at 405 nm. Pellets, prepared as described above, were thawed and resuspended using a Polytron homogenizer in an enzyme assay buffer containing 50 mM Tris-HCl (pH 7.4), 140 mM NaCl, 0.1% (w/v) BSA and 100  $\mu$ M phenyl methyl sulfonyl fluoride. The incubation mixture comprised 50  $\mu$ l membrane homogenate, 200  $\mu$ l L-Leu-pNA (1.5 mM) and 50  $\mu$ l enzyme assay buffer alone or with the test compound. The amount of membrane homogenate corresponded to  $4 \times 10^5$  CHO-K1 cells and  $1.5 \times 10^5$  transfected HEK293 cells in each well. Assays were carried out at 37 °C in 96-well plates (Medisch Labo Service, Menen, Belgium), and the formation of *p*-nitroaniline was followed by measuring the absorption at 405 nm every 5 min between 10 and 50 min in a Bio-Whittaker ELISA reader. The enzymatic activities were calculated by linear regression analysis of the timewise increase of the absorption.

## Radioligand Binding Assays

The binding affinities of Ang IV and of compounds **2–11** (Table 1) were assessed using porcine frontal cortex membranes. The binding of [<sup>125</sup>I] Ang IV to frontal cortex membranes (60  $\mu$ g of protein) was conducted in a final volume of 500  $\mu$ l binding buffer containing 50 mM Tris-HCl (pH 7.4), 150 mM NaCl, 5 mM EDTA, 0.1% BSA (w/v), 100  $\mu$ M PMSF, 20  $\mu$ M bestatin, 0.05 nM [<sup>125</sup>I] Ang IV and variable concentrations of the test substance. The samples were incubated for 2 h (37 °C) and the binding was terminated by filtration through Whatman GF/B glass fiber filters (presoaked in 0.3% polyethylenimine for 20 h) using a Brandel cell harvester. The filters were washed with  $4 \times 2$  ml of 50 mM Tris-HCl (pH 7.4), containing 150 mM NaCl and 5 mM EDTA and the radioactivity was subsequently measured in a gamma counter. Nonspecific binding was determined in the presence of 1  $\mu$ M unlabeled Ang IV. All experiments were performed in triplicate.

The stability of Ang IV and compound **4** was compared in the presence of CHO-K1 cell membranes. Membrane pellets were thawed and resuspended using a Polytron homogenizer in 50 mM Tris-HCl (pH 7.4) enzyme assay buffer and the assays were carried out in polyethylene 24-well plates (Elscolab, Kruikebeke, Belgium). Preincubations were carried out for 40 min at 37 °C in 250  $\mu$ l containing 150  $\mu$ l membrane homogenate, 50  $\mu$ l enzyme assay buffer without or with 30 mM EDTA/600  $\mu$ M 1,10-Phe and 50  $\mu$ l enzyme assay buffer without or with compound **4** or unlabeled Ang IV (60  $\mu$ M for nonspecific binding). Then the binding assay was initiated by adding 50  $\mu$ l enzyme assay buffer containing [<sup>125</sup>I] Ang IV (without or with 30 mM EDTA/600  $\mu$ M 1,10-Phe) and the mixture was further incubated for 30 min at 37 °C. Final membrane concentrations were the same as for the enzyme assays, final chelator concentrations (when present) were 5 mM EDTA and 100  $\mu$ M 1,10-Phe, the final [<sup>125</sup>I] Ang IV concentration was 1 nM, and the final unlabeled ligand concentrations are indicated in Figure 2. After incubation, the mixture was vacuum-filtered using a Inotech 24-well cell harvester through GF/B glass fiber filters (Whatman) presoaked in 1% (w/v) BSA. After drying, the radioactivity retained in the filters was measured using a Perkin-Elmer  $\gamma$ -counter.

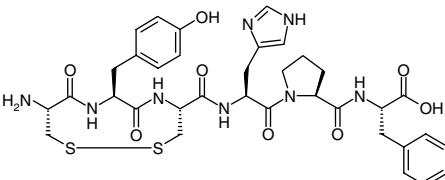
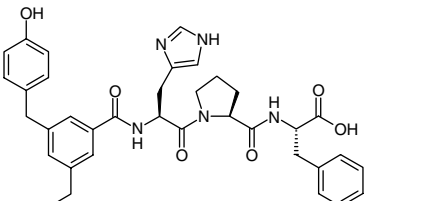
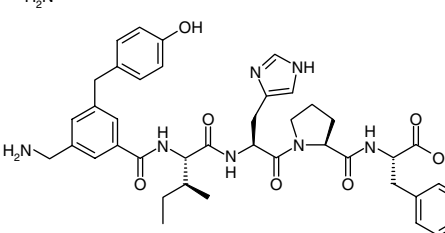
**Table 1** Chemical structures and the binding affinity of the compounds synthesized

Substance	No.	K <sub>i</sub> (nM)
	<b>1</b>	4.6 (IC <sub>50</sub> )
	<b>2</b>	6.5
	<b>3</b>	10.0
	<b>4</b>	1.9
	<b>5</b>	9.7
	<b>6</b>	37.6
	<b>7</b>	69.7
	<b>8</b>	42.0

## Data Analysis

All experiments were performed at least 3 times with duplicate determinations each. The calculation of IC<sub>50</sub> values from competition binding (or enzyme inhibition) experiments were performed by nonlinear regression analysis using GraphPad

**Table 1** (Continued)

Substance	No.	$K_i$ (nM)
	<b>9</b>	5000
	<b>10</b>	> 10 000
	<b>11</b>	2180

Prism 4.0. The equilibrium dissociation constants ( $K_i$  values) of the tested compounds in the binding and enzyme assays were calculated using the equation  $K_i = \{IC_{50}/(1 + [L]/K)\}$  in which [L] is the concentration of free radioligand (binding) or free substrate concentration (enzyme assay) and  $K$  the equilibrium dissociation constant ( $K_D$ ) of [ $^{125}I$ ] Ang IV (from saturation binding experiments) or the Michaelis–Menten constant ( $K_m$ ) for substrate cleavage [43].

## RT-PCR

The anterior lateral ventricle wall of 5–6-week-old mice was dissected for either RNA isolation or neurospheres preparation as stated above, in which case the neurospheres were harvested for RNA preparation 3 days after the first split. Total RNA was isolated using RNeasy Mini Kit (Qiagen) according to the manufacturer's instructions and DNase treated with DNase I (Ambion) according to protocol. A one-step RT-PCR Kit with Platinum Taq (Invitrogen) was used to detect the presence of IRAP mRNA. Briefly, 12.5 ng of total RNA was used in each 30-cycle reaction, with primers 5'-TGA GTG ACA AAG ACC GAG CCA-3' and 5'-ACC TTG AAC ACA GTG ACC ATG ACA-3' at an annealing temperature of 55 °C, generating a 431-base pair PCR product. To ensure that genomic DNA contamination did not give rise to false positive results, an identical reaction was carried out in which the RT-Taq polymerase mix was replaced by Taq polymerase alone and run in parallel with the experimental RT-PCR. The PCR product was run on a 1.5% TBE gel with ethidium bromide and the band of the correct size was cut out and cleaned with QIA quick Gel Extraction Kit (Qiagen). The band was re-amplified for sequencing, which was done using an ABI Prism Big Dye Terminator Cycle Sequencing Ready Reaction Kit (Applied Biosystems). The

resulting sequence confirmed the specificity of the RT-PCR reaction.

**Mouse Neural Stem Cell Proliferation Assay.** Mouse primary neural stem cell cultures were prepared as previously described [44]. Briefly, adult mouse brain subventricular zones were dissected and dissociated. Cells were cultured in suspension in DMEM/F12 supplemented with 2% B27, 10 ng/ml EGF, 10 ng/ml FGF-2 and penicillin–streptomycin, forming characteristic neurospheres (reagents Invitrogen). Cell proliferation was assayed using a BrdU ELISA Cell Proliferation kit (Roche cat 11 669 915 001). BrdU is a nucleotide analog that is incorporated into the genomic DNA during the S-phase. Immunochemical detection of incorporated BrdU can be used to quantitate cell proliferation [45–47]. Briefly, neurospheres (passage 3) were dissociated with trypsin–EDTA and the cells were seeded on poly-D-lysine coated plates and allowed to adhere overnight at 37 °C in a 5% CO<sub>2</sub> incubator. The following day, test compound(s) were added and incubation continued for additional 48 h. BrdU was added to a final concentration of 1  $\mu$ M and incubation was continued for an additional 24 h. Cells were fixed and the bound BrdU was quantitated according to kit instructions using peroxidase-labeled anti-BrdU antibodies and a chemiluminescent substrate. Statistical analysis was one-way ANOVA followed by Dunnett's post-test compared to untreated control performed in GraphPad 4.0.

**Conformational Energy Calculations.** The calculations were performed using the OPLS.2005 force field as implemented in the program MacroModel 9.1 (Schrödinger, LLC, New York, NY, 2005) essentially as reported previously [48]. The General Born Solvent Accessible (GB/SA) surface area method for water developed by Still [49] was used in all calculations. The number of torsion angles allowed to vary simultaneously during each Monte Carlo step ranged from 1 to ( $n - 1$ ) where  $n$  equals the total number of rotatable bonds. Amide bonds were fixed in the *trans* configuration. Conformational searches were conducted by use of the systematic unbound multiple minimum (SUMM) search method [50] in the batchmin program (command SPMC). Twenty thousand step runs were performed and those conformations within 50 kJ/mol of the global minimum were kept. Torsional memory and geometrical preoptimization were used. Truncated Newton conjugated gradient (TNCG) minimization was used in the conformational search with derivative convergence set to 0.001 (kJ/mol)/Å.

## RESULTS

In order to determine the importance of the C-terminal carboxylate group of Ang IV analogs for their binding affinity to the IRAP/AT<sub>4</sub> receptor in porcine frontal cortex membranes, the N-terminally acetylated peptide **3** was first examined. This peptide was found to exhibit approximately half of the potency of Ang IV (**1**). Therefore, we decided to retain the carboxylate group in the new compounds we prepared and to replace the cyclic system of **2** with various properly substituted benzoic acids and phenylacetic acids. The chemical structures and the binding affinity of the compounds synthesized are shown in Table 1. The initial molecular modeling suggested that compounds

**4–7** could place the carboxylate group of the turn mimetic in approximately the same space as the C-terminal carboxylate of **2** when it adopts a  $\gamma$ -turn centered around Pro. Indeed, all compounds in the series showed reasonable affinity. Compound **4** exhibited the best binding affinity, presenting a  $K_i$  value of 1.9 nM. Migration of the side chain to the *m*-position of the aromatic ring rendered a ligand (**5**) with a  $K_i$  value of 9.7 nM, and subsequent deletion of the methylene group of **5** gave the benzoic acid derivative **6** displaying a  $K_i$  value of 37.6 nM. The *p*-substituted arylacetic acid derivative **7** was less active and exhibited a  $K_i$  of 69.7 nM. Replacement of the aromatic scaffold of the latter compound by four methylene groups delivered the saturated and flexible **8**, characterized by the long tether arm. This aliphatic carboxylic acid derivative was equipotent to **6**.

With regard to the N-terminal of Ang IV, we previously demonstrated that cysteine cyclization between position 1 and position 3 of Ang IV, enclosing Tyr<sup>2</sup> in the ring system, resulted in a poor ligand (**9**) with a  $K_i$  of 5000 nM [31]. Likewise, neither was the incorporation of an aromatic scaffold to mimic a tentative turn of the backbone centered at Tyr<sup>2</sup> a fruitful operation. Compound **10** did not display measurable binding affinity. However, ligand **11**, in which the Ile residue is retained, still displayed affinity, albeit weak, to the IRAP/AT<sub>4</sub> receptor ( $K_i = 2180$  nM).

### Conformational Analysis

Conformational analysis was performed on model compounds of **2** and **4–8**. The model compounds were built by substituting the Val-Tyr-Ile fragment in all compounds for an acetyl group. The OPLS-AA force field and the GB/SA water solvation model within MacroModel (version 9.1) were used in the calculations. The number of conformations within 5 kcal/mol of the global energy minimum found for the model compounds of **2**, **4**, **5**, **6**, **7** and **8** were 63, 20, 27, 11, 18 and 703, respectively. The third lowest energy conformation identified of **2** ( $\Delta E = 0.23$  kcal/mol), which adopted an inverse  $\gamma$ -turn, was used as the template in all comparisons.

### Mouse Neural Stem Cell Proliferation

The presence of IRAP/AT<sub>4</sub> receptor mRNA in cultured mouse adult neural stem cells and in the lateral ventricle wall of adult mice was detected using RT-PCR. The reaction produced a band of expected size, which was unambiguously identified by sequencing. The risk of a false positive result due to genomic DNA contamination is minimal because a parallel control with no reverse transcriptase was negative and primers that span two large introns were used in the experiment.

The most potent ligand in the series, compound **4**, was tested in a mouse neural stem cell proliferation assay in three doses (1, 10 and 100 nM). A statistically significant ( $9 < 0.01$ ) effect was seen with the highest dose (Figure 4).

### Enzyme Activity

Compound **4** was compared with the disulfide **2** for its ability to inhibit the catalytic activity of recombinant human IRAP and AP-N, transiently transfected in HEK293 cells; and of IRAP natively expressed in CHO-K1 cells (Figure 1, Table 2). As described previously, the enzymatic activity was assessed spectrophotometrically by measuring the absorption of *p*-nitroaniline (i.e. the cleavage product of the synthetic substrate L-Leu-pNA) at 405 nm over time at 37°C [26]. The corresponding rate constants (further denoted as enzymatic activities) were calculated by linear regression analysis of the timewise increase of the absorption.

The two derivatives **2** and **4** were competitive with the substrate (data not shown) and displayed monophasic inhibition curves (Figure 1). Their  $pK_i$  values, as calculated by the Cheng and Prusoff equation (1973) from their IC<sub>50</sub> values and  $K_m$  values of L-Leu-pNA for the different enzyme preparations, are listed in Table 2. Both compounds displayed similar inhibition characteristics, and they inhibited the activity of recombinant and endogenous IRAP more potently than recombinant AP-N. Whereas both compounds displayed similar potency for IRAP, the disulfide **2** was slightly more potent for AP-N.

### Stability Experiments with (<sup>125</sup>I) Ang IV Binding

As earlier observed for compound **2** and Ang IV [31], compound **4** produced monophasic inhibition curves of [<sup>125</sup>I] Ang IV binding to CHO-K1 cell membranes (30 min incubation at 37°C with 1 nM radioligand)

**Table 2** Inhibition of enzyme activity by compounds **2** and **4**

	Compound <b>2</b>	Compound <b>4</b>
CHO-K1	50.6 ± 14.7	55.8 ± 8.9
HEK293 + IRAP	25.8 ± 3.2	43.6 ± 1.5
HEK293 + AP-N	221.9 ± 28.1	951.0 ± 84.8

$K_i$  values (nM) were calculated according to the Cheng and Prusoff equation using IC<sub>50</sub> values and the  $K_m$  values for L-Leu-pNA from recombinant IRAP (0.25 ± 0.05 mM), recombinant AP-N (0.41 ± 0.02 mM) and endogenous IRAP in CHO-K1 cells (0.39 ± 0.04 mM) [25]. Data (illustrated in Figure 2 for compound **4**) are the mean ± standard error of mean (SEM) of three independent experiments. Data for compound **2** are from Ref. 31.

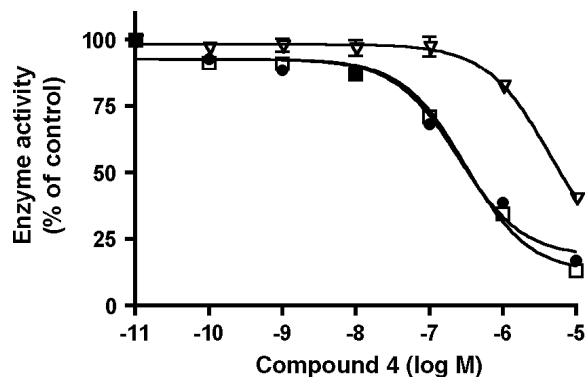


**Figure 1** Inhibition of the enzymatic activity by compound **4**. Membranes of HEK293 cells transfected with human IRAP ( $\square$ ) or human AP-N ( $\Delta$ ) (corresponding to  $1.5 \times 10^5$  cells/incubation) and CHO-K1 cells ( $\bullet$ ) (corresponding to  $4 \times 10^5$  cells/incubation) were incubated at  $37^\circ\text{C}$  with  $1.5 \text{ mM}$  L-Leu-pNA in the absence (control activity) or the presence of increasing concentrations of compound. The rate constants of L-Leu-pNA cleavage ( $v$ , corresponding to enzyme activity and expressed as a percentage of control) were calculated by linear regression analysis of the absorption (at  $405 \text{ nm}$ ) versus time curves with measurements made every  $5 \text{ min}$  (between  $10$  and  $50 \text{ min}$ ). The  $K_i$  values of these peptides are given in Table 2.

(Figure 2). To detect binding activity, these studies needed to be performed in the presence of the EDTA and 1.10-Phe, chelators which are known to effectively prevent metalloprotease activity [51]. To compare the susceptibility of **2**, **4** and Ang IV to metalloprotease-dependent breakdown, CHO-K1 cell membranes were preincubated with increasing concentrations of each compound for  $40 \text{ min}$  at  $37^\circ\text{C}$  either in the presence or in the absence of EDTA and 1.10-Phe before the binding assay. EDTA and 1.10-Phe preincubation produced a marked leftward shift of the Ang IV inhibition curve (Table 3), suggesting that this compound was rapidly degraded by IRAP and/or other metalloproteases present on the CHO-K1 cell membranes. In contrast, a much smaller shift was observed for **2** and **4** (Figure 2, Table 3), indicating that both compounds are more stable than Ang IV.

## DISCUSSION

The major objective of our research efforts is to identify small drug-like molecules that efficiently interact with the IRAP/AT<sub>4</sub> receptor. Such compounds could serve as leads for subsequent optimization processes aimed at developing new types of pharmaceuticals with the capacity to improve memory. Successful drug candidates that are orally absorbed and can cross the blood-brain barrier are not likely to be peptidic in character, unless the compounds utilize or rely on, e.g., peptide transporter systems for active membrane transport. Our ambition is to stepwise eliminate as

**Table 3** [ $^{125}\text{I}$ ] Ang IV competition binding in CHO-K1 membranes after preincubation in the absence or presence of EDTA and 1,10-phenanthroline (chelators)

IC <sub>50</sub> (nM)	No chelators	Chelators
Compound <b>2</b>	$203.5 \pm 144.9$	$28.7 \pm 10.1$
Compound <b>4</b>	$204.3 \pm 122.3$	$28.3 \pm 11.7$
Angiotensin IV	$1079.3 \pm 606.6$	$17.6 \pm 4.5$

Data (illustrated in Figure 2 for compound **4**) are the mean  $\pm$  SEM of three independent experiments. Data for compound **2** and Ang IV are from Ref. 31.

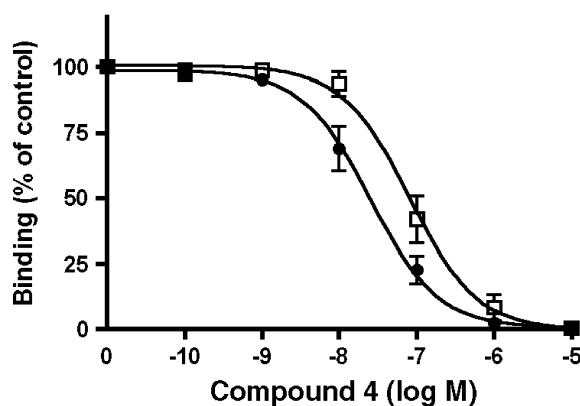


**Figure 2** Stability of compound **4** towards breakdown by metalloproteases present in CHO-K1 cell membranes. Membranes were preincubated for  $40 \text{ min}$  at  $37^\circ\text{C}$  with increasing concentrations of compound **4** in the presence ( $\bullet$ ) or absence ( $\square$ ) of EDTA and 1.10-phenanthroline before  $30 \text{ min}$  incubation with  $1 \text{ nM}$  [ $^{125}\text{I}$ ] Ang IV. Data refer to specific binding of [ $^{125}\text{I}$ ] Ang IV (expressed as percent of control binding in the absence of unlabeled compound), calculated by subtracting nonspecific binding in the presence of  $10 \mu\text{M}$  unlabeled Ang IV from total binding. Concentrations are the initial concentrations. The corresponding IC<sub>50</sub> values of these compounds are given in Table 3.

much as possible of the peptidic elements, including nonessential peptide bonds of identified IRAP/AT<sub>4</sub> receptor ligands. In order to determine the important pharmacophore elements of Ang IV and the relative positions of these elements in space, we recently prepared a series of constrained Ang IV analogs encompassing cyclic disulfide-containing ring systems [31]. This methodology to connect two residues of an acyclic peptide by disulfide formation is a well-established approach to obtain valuable structural information on bioactive conformations of peptides [52,53]. As hypothesized by us previously [31], compound **2** adopts in its C-terminal preferentially an inverse  $\gamma$ -turn, which is induced by the disulfide ring system [54].

The remarkably high potency of the *o*-phenylacetic acid derivative **4**, even more potent than **2**, provides



further support that Ang IV adopts a turn in its C-terminal region when binding to the IRAP/AT<sub>4</sub> receptor. As demonstrated in Figure 3, the carboxyl groups of energy-minimized conformers of **2** and **4** occupy similar positions. The modeling suggests that the *m*-phenylacetic acid derivative **5** is also able to localize its carboxylate in the same position as the corresponding carboxylate of **2** and **4** (Figure 3). It is also possible to position the C-terminal carboxylate groups of compounds **6–8** in similar positions as that of **2** (not shown). The lower affinities of compounds **6–8** are most likely attributed to a nonoptimal fit to the receptor. After the synthetic work of this investigation had been accomplished, we became aware of Japanese patents disclosing a series of related Ang IV receptor ligands modified at the C-terminal [55,56].

A  $\gamma$ -turn is unlikely to be adopted in the N-terminal part of Ang IV since **9**, **10** or **11** are not high-affinity ligands. The lack of the lipophilic side chain of Val<sup>1</sup> could account for this result since such chain in position 1 is known to have a highly favorable impact on the binding affinity of Ang IV for the IRAP/AT<sub>4</sub> receptor [27]. However, we have recently shown that the homocysteine homolog of **9** in fact exhibits a fair  $K_i$  value (i.e. 57 nM), implicating that the noncyclized lipophilic side chain is not crucial for binding and that it can be compensated for by an adequate lipophilic ring system [31]. Thus, we believe that more extended conformations are adopted by the hexapeptide Ang IV in the N-terminal or, alternatively, that a  $\beta$ -turn conformation is preferred in this region for optimal receptor recognition. Obviously, while it seems established that a  $\gamma$ -turn is adopted in the C-terminal, further research efforts are required for determining the bioactive conformation of the N-terminal region of Ang IV.

Compound **4** is considerably more drug-like than Ang IV itself and we found it to be a suitable candidate for further studies. Both compound **4** encompassing the

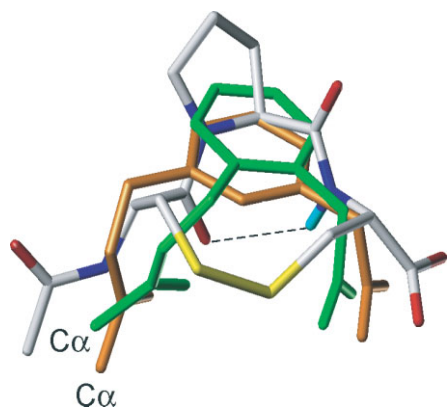


**Figure 3** Proposed bioactive conformation of the C-terminal region of angiotensin IV. The best fit of model compounds **4** (green) and **5** (orange) to compound **2** in a low-energy  $\gamma$ -turn conformation is shown. For clarity the hydrogen atoms are not displayed.

aromatic ring system in the C-terminal and the cyclic disulfide **2** inhibit the catalytic activity of recombinant human IRAP and AP-N, transiently transfected in HEK293 cells; and of IRAP natively expressed in CHO-K1 cells (Table I). The  $K_i$  values of both compounds for inhibiting IRAP activity are very similar to those previously determined for Ang IV (recombinant IRAP:  $K_i = 62.4 \pm 17.5$  nM, endogenous IRAP in CHO-K1 cells:  $K_i = 161.2 \pm 35.0$  nM). Both compounds display somewhat lower potency for inhibiting recombinant AP-N activity (5- to 9-fold for **2** and 17- to 21-fold for **4**). Similarly, Ang IV also displays lower potency for inhibiting recombinant AP-N activity ( $K_i = 841.4 \pm 37.8$  nM) [25].

The degradation of the disulfide **2** was previously assessed by us [31]. To compare the potential breakdown of **2**, **4** and Ang IV by metalloproteases, CHO-K1 cell membranes were preincubated with increasing concentrations of each compound either in the presence or in the absence of the chelators EDTA and 1.10-Phe before the binding assay with [<sup>125</sup>I] Ang IV (in the presence of EDTA and 1.10-Phe). EDTA and 1.10-Phe are well known for their ability to block IRAP, AP-N and other metalloproteinase activity [57] and, when present in the preincubation, they produced a marked leftward shift of the Ang IV inhibition curve (Table 3). This observation suggests that Ang IV is rapidly degraded by metalloproteases present in the CHO-K1 cell membranes. By contrast, a much smaller shift was observed for **2** and **4** (Table 3), indicating that the two conformationally constrained analogs are significantly more stable than Ang IV.

The proliferation of adult mouse neural stem cells *in vitro* was found to be stimulated by the addition of compound **4** to the media (Figure 4). The presence of the IRAP mRNA in the neural stem cells lends some support to the notion that the effect of compound **4** could be mediated via the IRAP protein. The proliferative effect could be mediated by inhibition of protease activity of IRAP, which could lead to accumulation of substrate peptides, or through direct IRAP signaling via intracellular cascades. However, to conclusively elucidate the molecular mechanism through which compound **4** exerts its action on the neural stem cells would require more extensive studies.

## CONCLUSIONS

In summary, a series of pseudopeptides containing aromatic scaffolds mimicking and substituting parts of the backbone of Ang IV have been synthesized and evaluated in biological assays. Several of the ligands displayed high affinity for the insulin-regulated membrane aminopeptidase (IRAP)/AT<sub>4</sub> receptor. Displacement of the C-terminal end Ang IV with an *o*-substituted arylacetic acid derivative delivered a ligand (**4**) that

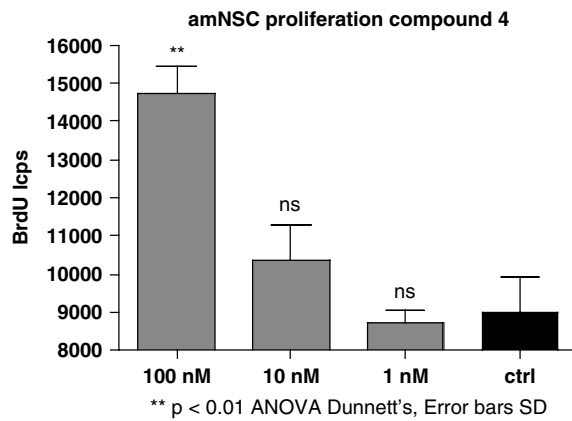


**Figure 4** Stimulation of adult mouse neural stem cell proliferation by compound **4**. In comparison to an untreated control, a significant increase ( $p < 0.01$ ) in BrdU incorporation, indicative of increased proliferation, was observed when the cells were stimulated with 100 nM of compound **4**. The lower concentrations tested (1 and 10 nM) had no significant effect.

exhibited the highest binding affinity (1.9 nM). This fact provides support to the hypothesis that Ang IV adopts a  $\gamma$ -turn in the C-terminal in its bioactive conformation. Ligand **4** inhibits both human cystine aminopeptidase and AP-N and, in addition, it was found to induce proliferation of adult neural stem cells. This ligand is degraded considerably more slowly in membrane preparations than Ang IV. As it has a lower molecular weight and is more drug-like than Ang IV, we believe that compound **4** might constitute a suitable research tool, in particular, in connection with more advanced studies of the role of Ang IV *in vivo*.

## Acknowledgements

We thank The Swedish Research Council, the Research Council of the 'Vrije Universiteit Brussel' (GOA-2002), the 'Geneeskundige Stichting Koningin Elisabeth' and the Institute for the Promotion of Innovation through Science and Technology in Flanders (I.W.T.-Vlaanderen) for financial support.

## REFERENCES

- Hallberg M, Le Greves P, Nyberg F. Neuropeptide processing. In *Proteases in Biology and Disease, Proteases in the brain*, Vol. 3, Lendeckel U, Hooper NM (ed.). Springer Science: New York, 2005; 203–234.
- Hallberg M, Nyberg F. Neuropeptide conversion to bioactive fragments – an important pathway in neuromodulation. *Curr. Protein Pept. Sci.* 2003; **4**: 31–44.
- Vauquelin G, Michotte Y, Smolders I, Sarre S, Ebinger G, Dupont A, Vanderheyden P. Cellular targets for angiotensin II fragments: pharmacological and molecular evidence. *J. Renin. Angiotensin Aldosterone Syst.* 2002; **3**: 195–204.
- von Bohlen und Halbach O. Angiotensin IV in the central nervous system. *Cell Tissue Res.* 2003; **311**: 1–9.
- Chai SY, Fernando R, Peck G, Ye SY, Mendelsohn FA, Jenkins TA, Albiston AL. The angiotensin IV/AT4 receptor. *Cell. Mol. Life Sci.* 2004; **61**: 2728–2737.
- Braszko JJ, Kupryszewski G, Witczuk B, Wisniewski K. Angiotensin II-(3–8)-hexapeptide affects motor activity, performance of passive avoidance and a conditioned avoidance response in rats. *Neuroscience* 1988; **27**: 777–783.
- Wright JW, Miller-Wing AV, Shaffer MJ, Higginson C, Wright DE, Hanesworth JM, Harding JW. Angiotensin II(3–8) (ANG IV) hippocampal binding: potential role in the facilitation of memory. *Brain Res. Bull.* 1993; **32**: 497–502.
- Wright JW, Stubbley L, Pederson ES, Kramar EA, Hanesworth JM, Harding JW. Contributions of the brain angiotensin IV-AT4 receptor subtype system to spatial learning. *J. Neurosci.* 1999; **19**: 3952–3961.
- Delorenzi A, Locatelli F, Romano A, Nahmod V, Maldonado H. Angiotensin II (3–8) induces long-term memory improvement in the crab *Chasmagnathus*. *Neurosci. Lett.* 1997; **226**: 143–146.
- Delorenzi A, Maldonado H. Memory enhancement by the angiotensinergic system in the crab *Chasmagnathus* is mediated by endogenous angiotensin II. *Neurosci. Lett.* 1999; **266**: 1–4.
- Pederson ES, Harding JW, Wright JW. Attenuation of scopolamine-induced spatial learning impairments by an angiotensin IV analog. *Regul. Pept.* 1998; **74**: 97–103.
- Pederson ES, Krishnan R, Harding JW, Wright JW. A role for the angiotensin AT4 receptor subtype in overcoming scopolamine-induced spatial memory deficits. *Regul. Pept.* 2001; **102**: 147–156.
- Lee J, Albiston AL, Allen AM, Mendelsohn FA, Ping SE, Barrett GL, Murphy M, Morris MJ, McDowall SG, Chai SY. Effect of I.C.V. injection of AT4 receptor ligands, NLE1-angiotensin IV and LVV-hemorphin 7, on spatial learning in rats. *Neuroscience* 2004; **124**: 341–349.
- Hall KL, Venkateswaran S, Hanesworth JM, Schelling ME, Harding JW. Characterization of a functional angiotensin IV receptor on coronary microvascular endothelial cells. *Regul. Pept.* 1995; **58**: 107–115.
- Swanson GN, Hanesworth JM, Sardinia MF, Coleman JK, Wright JW, Hall KL, Miller-Wing AV, Stobb JW, Cook VI, Harding EC, et al. Discovery of a distinct binding site for angiotensin II (3–8), a putative angiotensin IV receptor. *Regul. Pept.* 1992; **40**: 409–419.
- Albiston AL, McDowall SG, Matsacos D, Sim P, Clune E, Mustafa T, Lee J, Mendelsohn FA, Simpson RJ, Connolly LM, Chai SY. Evidence that the angiotensin IV (AT4) receptor is the enzyme insulin-regulated aminopeptidase. *J. Biol. Chem.* 2001; **276**: 48623–48626.
- Rogi T, Tsujimoto M, Nakazato H, Mizutani S, Tomoda Y. Human placental leucine aminopeptidase/oxytocinase. A new member of type II membrane-spanning zinc metallopeptidase family. *J. Biol. Chem.* 1996; **271**: 56–61.
- Albiston AL, Mustafa T, McDowall SG, Mendelsohn FA, Lee J, Chai SY. AT4 receptor is insulin-regulated membrane aminopeptidase: potential mechanisms of memory enhancement. *Trends Endocrinol. Metab.* 2003; **14**: 72–77.
- Wright JW, Harding JW. The brain angiotensin system and extracellular matrix molecules in neural plasticity, learning, and memory. *Prog. Neurobiol.* 2004; **72**: 263–293.
- Kramar EA, Harding JW, Wright JW. Angiotensin II- and IV-induced changes in cerebral blood flow. Roles of AT1, AT2, and AT4 receptor subtypes. *Regul. Pept.* 1997; **68**: 131–138.
- Handa RK, Krebs LT, Harding JW, Handa SE. Angiotensin IV AT4-receptor system in the rat kidney. *Am. J. Physiol.* 1998; **274**: F290–F299.
- Handa RK. Characterization and signaling of the AT(4) receptor in human proximal tubule epithelial (HK-2) cells. *J. Am. Soc. Nephrol.* 2001; **12**: 440–449.
- Chen JK, Zimpelmann J, Harris RC, Burns KD. Angiotensin IV induces tyrosine phosphorylation of focal adhesion kinase and

- paxillin in proximal tubule cells. *Am. J. Physiol. Renal Physiol.* 2001; **280**: F980–F988.
24. Li YD, Block ER, Patel JM. Activation of multiple signaling modules is critical in angiotensin IV-induced lung endothelial cell proliferation. *Am. J. Physiol. Lung Cell Mol. Physiol.* 2002; **283**: L707–L716.
  25. Demaegdts H, Lenaerts PJ, Swales J, De Backer JP, Laeremans H, Le MT, Kersemans K, Vogel LK, Michotte Y, Vanderheyden P, Vauquelin G. Angiotensin AT<sub>4</sub> receptor ligand interaction with cystinyl aminopeptidase and aminopeptidase N: [125I]Angiotensin IV only binds to the cystinyl aminopeptidase apo-enzyme. *Eur. J. Pharmacol.* 2006; **546**: 19–27.
  26. Demaegdts H, Vanderheyden P, De Backer JP, Mosselmans S, Laeremans H, Le MT, Kersemans V, Michotte Y, Vauquelin G. Endogenous cystinyl aminopeptidase in Chinese hamster ovary cells: characterization by [125I]Ang IV binding and catalytic activity. *Biochem. Pharmacol.* 2004; **68**: 885–892.
  27. Sardinia MF, Hanesworth JM, Krebs LT, Harding JW. AT<sub>4</sub> receptor binding characteristics: D-amino acid- and glycine-substituted peptides. *Peptides* 1993; **14**: 949–954.
  28. Sardinia MF, Hanesworth JM, Krishnan F, Harding JW. AT<sub>4</sub> receptor structure-binding relationship: N-terminal-modified angiotensin IV analogues. *Peptides* 1994; **15**: 1399–1406.
  29. Krishnan R, Hanesworth JM, Wright JW, Harding JW. Structure-binding studies of the adrenal AT<sub>4</sub> receptor: analysis of position two- and three-modified angiotensin IV analogs. *Peptides* 1999; **20**: 915–920.
  30. Krebs LT, Kramar EA, Hanesworth JM, Sardinia MF, Ball AE, Wright JW, Harding JW. Characterization of the binding properties and physiological action of divalinal-angiotensin IV, a putative AT<sub>4</sub> receptor antagonist. *Regul. Pept.* 1996; **67**: 123–130.
  31. Axén A, Lindeberg G, Demaegdts H, Vauquelin G, Karlén A, Hallberg M. Cyclic insulin-regulated aminopeptidase (IRAP)/AT<sub>4</sub> receptor ligands. *J. Pept. Sci.* 2006; **12**: 705–713.
  32. Falk A, Frisen J. New neurons in old brains. *Ann. Med.* 2005; **37**: 480–486.
  33. Li J, Imitola J, Snyder EY, Sidman RL. Neural stem cells rescue nervous purkinje neurons by restoring molecular homeostasis of tissue plasminogen activator and downstream targets. *J. Neurosci.* 2006; **26**: 7839–7848.
  34. Pluchino S, Zanotti L, Rossi B, Brambilla E, Ottoboni L, Salani G, Martinello M, Cattalini A, Bergami A, Furlan R, Comi G, Constantin G, Martino G. Neurosphere-derived multipotent precursors promote neuroprotection by an immunomodulatory mechanism. *Nature* 2005; **436**: 266–271.
  35. Barlos K, Gatos D, Kallitsis J, Papaphotiu G, Sofiriu P, Yao WQ, Schafer W. Synthesis of protected peptide-fragments using substituted triphenylmethyl resins. *Tetrahedron Lett.* 1989; **30**: 3943–3946.
  36. Lahoutte T, Mertens J, Caveliers V, Franken PR, Everaert H, Bossuyt A. Comparative biodistribution of iodinated amino acids in rats: selection of the optimal analog for oncologic imaging outside the brain. *J. Nucl. Med.* 2003; **44**: 1489–1494.
  37. Tang ZL, Pelletier JC. Preparation of amides from acids and resin bound azides: suppression of intramolecular lactam formation. *Tetrahedron Lett.* 1998; **39**: 4773–4776.
  38. Xu J, Guo Z. (2-Azidomethyl)phenylacetyl as a new, reductively cleavable protecting group for hydroxyl groups in carbohydrate synthesis. *Carbohydr. Res.* 2002; **337**: 87–91.
  39. Lindman S, Lindeberg G, Nyberg F, Karlen A, Hallberg A. Comparison of three gamma-turn mimetic scaffolds incorporated into angiotensin II. *Bioorg. Med. Chem. Lett.* 2000; **8**: 2375–2383.
  40. Johansen TE, Scholler MS, Tolstoy S, Schwartz TW. Biosynthesis of peptide precursors and protease inhibitors using new constitutive and inducible eukaryotic expression vectors. *FEBS Lett.* 1990; **267**: 289–294.
  41. Olsen J, Cowell GM, Königshofer E, Danielsen EM, Møller J, Laustsen L, Hansen OC, Welinder KG, Engberg J, Hunziker W, Spiess M, Sjöström H, Norén O. Complete amino acid sequence of human intestinal aminopeptidase N as deduced from cloned cDNA. *FEBS Lett.* 1988; **238**: 307–314.
  42. Le MT, De Backer JP, Hunyady L, Vanderheyden PM, Vauquelin G. Ligand binding and functional properties of human angiotensin AT<sub>1</sub> receptors in transiently and stably expressed CHO-K1 cells. *Eur. J. Pharmacol.* 2005; **513**: 35–45.
  43. Cheng Y, Prusoff WH. Relationship between the inhibition constant (K<sub>i</sub>) and the concentration of inhibitor which causes 50 per cent inhibition (I<sub>50</sub>) of an enzymatic reaction. *Biochem. Pharmacol.* 1973; **22**: 3099–3108.
  44. Mercer A, Ronnholm H, Holmberg J, Lundh H, Heidrich J, Zachrisson O, Ossoinak A, Frisen J, Patrone C. PACAP promotes neural stem cell proliferation in adult mouse brain. *J. Neurosci. Res.* 2004; **76**: 205–215.
  45. Morstyn G, Pyke K, Gardner J, Ashcroft R, de Fazio A, Bhathal P. Immunohistochemical identification of proliferating cells in organ culture using bromodeoxyuridine and a monoclonal antibody. *J. Histochem. Cytochem.* 1986; **34**: 697–701.
  46. Gratzner HG. Monoclonal antibody to 5-bromo- and 5-iododeoxyuridine: a new reagent for detection of DNA replication. *Science* 1982; **218**: 474–475.
  47. Crissman HA, Steinkamp JA. A new method for rapid and sensitive detection of bromodeoxyuridine in DNA-replicating cells. *Exp. Cell Res.* 1987; **173**: 256–261.
  48. Lindman S, Lindeberg G, Gogoll A, Nyberg F, Karlen A, Hallberg A. Synthesis, receptor binding affinities and conformational properties of cyclic methylenedithioether analogues of angiotensin II. *Bioorg. Med. Chem.* 2001; **9**: 763–772.
  49. Still WC, Tempczyk A, Hawley RC, Hendrickson T. Semianalytical treatment of solvation for molecular mechanics and dynamics. *J. Am. Chem. Soc.* 1990; **112**: 6127–6129.
  50. Goodman JM, Still WC. An unbounded systematic search of conformational space. *J. Comput. Chem.* 1991; **12**: 1110–1117.
  51. Lowther WT, Matthews BW. Metalloaminopeptidases: common functional themes in disparate structural surroundings. *Chem. Rev.* 2002; **102**: 4581–4608.
  52. Spear KL, Brown MS, Reinhard EJ, McMahon EG, Olins GM, Palomo MA, Patton DR. Conformational restriction of angiotensin II: cyclic analogues having high potency. *J. Med. Chem.* 1990; **33**: 1935–1940.
  53. Schiller PW, Eggmann B, DiMaio J, Lemieux C, Nguyen TM. Cyclic enkephalin analogs containing a cystine bridge. *Biochem. Biophys. Res. Commun.* 1981; **101**: 337–343.
  54. Schmidt B, Lindman S, Tong W, Lindeberg G, Gogoll A, Lai Z, Thornwall M, Synnergren B, Nilsson A, Welch CJ, Sohtell M, Westerlund C, Nyberg F, Karlen A, Hallberg A. Design, synthesis, and biological activities of four angiotensin II receptor ligands with gamma-turn mimetics replacing amino acid residues 3–5. *J. Med. Chem.* 1997; **40**: 903–919.
  55. Kobori T, Goda K, Sugimoto K, Ota T, Tomisawa K. *Preparation of Peptide Derivatives as Angiotensin IV Receptor Agonists*. WO 97/03093 A1 1997.
  56. Kobori T, Goda K, Sugimoto K, Ota T, Tomisawa K. *Preparation of Amino Acid Derivatives as Angiotensin IV Receptor Agonists*. WO 98/05624 A1 1998.
  57. Irons DW, Davison JM, Baylis PH. Evaluation of enzyme inhibitors of cystinyl aminopeptidase and application to the measurement of immunoreactive atrial natriuretic peptide in human pregnancy. *Clin. Chim. Acta* 1994; **231**: 185–191.